



Glycinebetaine mitigates tomato chilling stress by maintaining high-cyclic electron flow rate of photosystem I and stability of photosystem II

Dandan Wei^{1,2} · Tianpeng Zhang¹ · Bingquan Wang³ · Huiling Zhang¹ · Mingyang Ma¹ · Shufen Li¹ · Tony H. H. Chen⁴ · Marian Brestic⁵ · Yang Liu¹ · Xinghong Yang¹

Received: 18 December 2021 / Accepted: 26 January 2022 / Published online: 12 February 2022
© The Author(s), under exclusive licence to Springer-Verlag GmbH Germany, part of Springer Nature 2022

Abstract

Key message Glycinebetaine alleviates chilling stress by protecting photosystems I and II in *BADH*-transgenic and GB-treated tomato plants, which can be an effective strategy for improving crop chilling tolerance.

Abstract Tomato (*Solanum lycopersicum*) is one of the most cultivated vegetables in the world, but is highly susceptible to chilling stress and does not naturally accumulate glycinebetaine (GB), one of the most effective stress protectants. The protective mechanisms of GB on photosystem I (PSI) and photosystem II (PSII) against chilling stress, however, remain poorly understood. Here, we address this problem through exogenous GB application and generation of transgenic tomatoes (Moneymaker) with a gene encoding betaine aldehyde dehydrogenase (BADH), which is the key enzyme in the synthesis of GB, from spinach. Our results demonstrated that GB can protect chloroplast ultrastructure, alleviate PSII photoinhibition and maintain PSII stability under chilling stress. More importantly, GB increased the electron transfer between Q_A and Q_B and the redox potential of Q_B and maintained a high rate of cyclic electron flow around PSI, contributing to reduced production of reactive oxygen species, thereby mitigating PSI photodamage under chilling stress. Our results highlight the novel roles of GB in enhancing chilling tolerance via the protection of PSI and PSII in *BADH* transgenic and GB-treated tomato plants under chilling stress. Thus, introducing GB-biosynthetic pathway into tomato and exogenous GB application are effective strategies for improving chilling tolerance.

Keywords Glycinebetaine · Photosynthesis · Photosystem I · Photosystem II · Cyclic electron transport · Chilling stress · Tomato

Introduction

Being a sessile organism, plants are frequently exposed to abiotic stresses, such as low and high temperature, drought, flooding, submergence, high light intensities and ultraviolet radiation during their lifetimes (Zhu 2016; Gong et al. 2020). The osmoprotection system is one of the most important

mechanism to survive various abiotic stresses in plants, which uses various low-molecular weight compounds called “compatible solutes” to alleviate the negative effect of abiotic stresses (Chen and Murata 2002, 2008, 2011). At present, numerous recent studies have investigated glycinebetaine (GB) as one of the most effective compatible solutes to increase plant tolerance against various types of environmental stresses (Zhang et al. 2020, 2021; Li et al. 2021a).

Chilling stress is one of the most serious abiotic stresses that limits the growth and development of plants and leads to negative effects on crop production and product quality (Ding et al. 2020; Gong et al. 2020; Zeng et al. 2021). As a nontoxic osmoprotectant, either the genetically engineered biosynthesis of GB or exogenous GB application can enhance chilling resistance (Park et al. 2006; Ming et al. 2021). Park et al. (2004, 2006) reported that exogenous GB application significantly increases chilling tolerance in

Communicated by Chun-Hai Dong.

Dandan Wei and Tianpeng Zhang contributed equally to this work.

✉ Yang Liu
liuy@sdau.edu.cn

✉ Xinghong Yang
xhyang@sdau.edu.cn

Extended author information available on the last page of the article

tomato seedlings, and this tolerance may be involved in the H_2O_2 -mediated antioxidant mechanisms in tomato plants. Likewise, in hybrid maize, seed treatments with GB can improve chilling tolerance by maintaining higher antioxidant activities and tissue water content, as well as reducing membrane electrolyte leakage (Farooq et al. 2008). Furthermore, the introduction of genes related to the GB biosynthetic pathway into non-GB synthesizing vegetables and crops, such as tomato (Park et al. 2004), has the potential to enhance the tolerance against various stress conditions, including low temperature (Chen and Murata 2011).

Oxygenic photosynthesis is the main process that drives life on earth. It starts with the harvesting of solar photons that, after transformation into electronic excitations, lead to charge separation in the reaction centers of photosystems I and II (PSI and PSII) (Croce and van Amerongen 2020). PSII is considered as a main part for photoinhibition when affected by abiotic stress (Nishiyama and Murata 2014; Huang et al. 2020), which always leads to an overreduction of electron transport chain (ETC) and causes photooxidation (Roach and Krieger-Liszka 2014; Sasi et al. 2018). Unlike PSII, PSI is not frequently damaged. However, once PSI is damaged, the recovery of photoinhibited PSI is very slow, and it has been reported in chilling-sensitive plants, such as tomatoes (Wang et al. 2018, 2020). Recent studies have shown that linear electron flow between PSII and PSI can be coordinated via the modulation of cyclic electron flow (CEF) under abiotic stresses (Yamori and Shikanai 2016; Huang et al. 2018; Wang et al. 2020), suggesting that CEF may play an important role in mitigating the photoinhibition of PSI under chilling stress.

As a low-molecular weight compound, GB can accumulate in the photosynthetic machinery, chloroplasts and plastids, at a high level during abiotic stresses (Chen and Murata 2011; Wei et al. 2017). Moreover, GB may protect photosynthetic machinery via stabilizing PSII complexes under salt and heat stress (Yang et al. 2005, 2007, 2008), as well as the resultant accelerated repair of photodamaged PSII, thereby contributing to maintaining photosynthesis activity (Murata et al. 2007; Li et al. 2021b).

GB plays an important role in enhanced chilling tolerance in plants under low-temperature stress (Park et al. 2004; 2006). Nevertheless, the roles of GB in the photoprotection of PSI and PSII during chilling stress remain poorly understood. In our study, we used *BADH* transgenic tomato plants and wild-type (WT, MoneyMaker) tomato plants applied with 5 mM GB to investigate the novel roles of GB in alleviating chilling-induced photoinhibition by (1) maintaining electron transformation between Q_A to Q_B , (2) increasing PSII complex stability, (3) increasing the rate of CEF around PSI and antioxidant enzymes, (4) increasing ATP content, and (5) accelerating D1 protein repairment; thereby, improving photosynthesis and enhancing chilling tolerance of PSI

and PSII in GB-accumulated tomato plants under chilling stress.

Materials and methods

Plant growth conditions and stress treatment

Tomato plants (*Solanum lycopersicum* MoneyMaker), WT and the *BADH* transgenic lines (line 10, line 28) (T4) were used in the experiments (Li et al. 2014). The tomato plants were grown under normal conditions at 25 °C/23 °C (day/night temperature), 400 $\mu\text{mol photons m}^{-2} \text{s}^{-1}$ photosynthetic photon flux density (PPFD), 75–80% relative humidity, and a photoperiod of 16/8 h (light/dark) in a greenhouse. After 5 weeks of growth, tomato seedlings were used for various experiments.

The WT plants were separated into two groups (WT and 5 mM GB-treated WT plants) each contained five plants and with three independent replicates. GB treatment was conducted according to Park et al. (2006), wherein 5 mM GB (WT + GB) was foliar applied to WT plants, and control plants were sprayed with water only. Tween-20 [0.005% (v/v)] was included as a wetting agent in all exogenous treatments and the GB-spraying treatment time is 3 days. After which, WT, transgenic lines (line 10, line 28) and WT + GB plants were transferred to 4 °C for 5 days in a cold growth chamber in the light (100 $\mu\text{mol photons m}^{-2} \text{s}^{-1}$). Next, they were transferred to a normal growth temperature condition and a PPFD of 400 $\mu\text{mol photons m}^{-2} \text{s}^{-1}$ and allowed to recover for 5 days. The third leaf from the bottom of the seedlings was used for the measurement of CO_2 assimilation, chlorophyll fluorescence, and other measurements.

Extraction and content determination of GB

GB was collected and detected as the method of Rhodes et al. (1989). Leaf samples (0.5 g) from *BADH* transgenic lines, WT and GB-treated WT tomatoes (WT + GB) were used in this experiment. The GB in the preliminarily tomato leaf extractions was analyzed by means of high-performance liquid chromatography (HPLC). Three biological replicates were used in each genotype.

Measurement of chlorophyll content

Eight fresh round leaves, obtained from each treatment, were mixed with 10 mL 95% ethanol. They were stored in the dark for 48 h for full extraction and then centrifuged at 3500g for 10 min. The absorbance of supernatant was determined at 663 nm and 646 nm with a UV/visible spectrophotometer (UV-2550, Shimadzu, Kyoto, Japan). Chlorophyll contents were determined as the method of Lichtenthaler and

Wellburn (1983). Three biological replicates were used in each genotype.

$$\text{Chlorophyll } a \ (C_a) = 12.21 \times D_{663} - 2.81 \times D_{646},$$

$$\text{Chlorophyll } b \ (C_b) = 20.13 \times D_{646} - 5.03 \times D_{663},$$

$$\text{Total chlorophyll} \ (C_T) = C_a + C_b = 17.32 \times D_{646} + 7.18 \times D_{663}.$$

Transmission electron microscopy (TEM)

After 5 days of control and chilling treatment, WT and transgenic tomato leaves were bladed in 4% glutaraldehyde (Electron Microscopy Sciences, Fort Washington, PA) for 24 h, fixed with 1% osmic acid for 4 h, and then dehydrated. They were embedded using Epon812, sliced by the LKB ultrathin slicer, stained with lead citrate and uranium dioxide acetate, and observed using a Jem-1400 electron microscope set at 80 kV. Images were captured with a CCD Camera (Philips Electronics, Eindhoven, The Netherlands).

Measurement of gas exchange in tomatoes

The gas exchange parameters of the third leaf from the bottom of the seedlings were detected by the CRIAS-2 Photosynthesis Measurements System (PP Systems International, Inc., Amesbury, MA, USA). They were separately measured at their saturated light intensity. Leaf temperature was 25 °C. Relative air humidity, ambient CO₂ concentration, and the determination of intensity were 85%, 380 μmol mol⁻¹, and a PPFD of 400 μmol m⁻² s⁻¹, respectively. Each measurement consists of three biological replicates.

Detection of the chlorophyll fluorescence

Chlorophyll fluorescence parameters were measured by FMS-2 (Hansatech Instruments Limited, Norfolk, UK) based on the following protocol. Modulated light (approximately 10 μmol m⁻² s⁻¹) was used to determine the minimal fluorescence (F_o) with all reaction centers open. And then, 0.3 s saturating light of 8000 μmol m⁻² s⁻¹ on a dark-adapted leaf (placed in the dark for 25 min) was utilized to determine the maximal fluorescence (F_m), which means all reaction centers were closed. The leaves were then light-adapted at consecutive light of 100 μmol m⁻² s⁻¹ and steady-state fluorescence (F_s) was read after 2 min illumination. The maximum fluorescence in the light-adapted state (F_m') was obtained after using an 0.8 s saturating light of 8000 μmol m⁻² s⁻¹. Tomato leaves were illuminated using a 3 s far-red light after the actinic light was turned off and then the minimum fluorescence in the light-adapted state (F_o') was measured.

Maximal photochemical efficiency (F_v/F_m) of PSII, photochemical quenching (q_p) and other parameters were calculated as follows: $F_v/F_m = (F_m - F_o)/F_m$; $q_p = (F_m' - F_o)/(F_m' - F_o')$; $\Phi_{PSII} = (F_m' - F_o')/F_m'$; $ETR = \Phi_{PSII} \times PPFD \times 0.5 \times 0.84$; $NPQ = F_m/F_m' - 1$.

To study the effect of GB on D1 protein repair, isolated function leaves were treated with or without 3 mM streptomycin sulfate (SM) at a PPFD of 100 μmol m⁻² s⁻¹ for 9 h, and F_v/F_m was determined using the above protocol before and after chilling treatment. Besides, diuron (DCMU) was used in this experiment and F_v/F_m was detected as the above methods. Each measurement consists of three biological replicates.

JIP test

To study the function of GB on linear electron transport chains, the chlorophyll *a* fluorescence transient (OJIP) curves were checked with a fluorometer Handy PEA (Hansatech Instruments Limited, Norfolk, UK) at normal temperature (25 °C). Chlorophyll fluorescence was measured on the third leaf from bottom of tomato seedlings. After adapted for 25 min, all parameters were detected. The experiments were completed on five plants from each repeat.

JIP test was analyzed using basic parameters calculated by chlorophyll *a* fluorescence transient data. Phenomenological fluxes on the level of the excited leaf cross-section (CS) [absorption (ABS/CS_m), trapping (TR_o/CS_m), dissipation (DI_o/CS_m), and electron transport (ET_o/SCm)] were calculated. The exciton efficiency of electron transport beyond Q_A was $\Psi_o = ET_o/TR_o = 1 - V_j$ (relative variable fluorescence at the J-step). These data were analyzed by Biolyzer 3.06 software. The detailed expression and terms applied in the JIP test for analysis of the chlorophyll fluorescence parameters are given in Table S2.

Measurements of 820 nm transmission

The Modulated Reflectance (MR) signal detected at 820 nm was conducted with M-PEA (Hansatech, UK) using the method described by Salvatori et al. (2014). It provided information regarding oxidation in PSI (including PC and P700). MR_o indicated the initial MR. After dark-adapted for 25 min, all samples were measured. The induction dynamics curve of MR₈₂₀ of tomato leaves was obtained by saturating red light, which showed a rapid oxidation phase and a reduction phase. The capability of P700 for oxidation was used to reflect the activity of PSI and it could be measured by the initial slope of oxidation phase of MR (Strasser et al. 2010).

There were two independent experiments for the measurement of the rate of CEF. First, whole tomato plants were exposed to 4 °C at a PPFD of 100 μmol m⁻² s⁻¹ chilling condition for 5 days and then recovered for another 5 days.

Second, isolated function leaves were treated with or without 0.02 mM iodoacetamide (IAM) subjected to chilling at a PPFD of 100 $\mu\text{mol m}^{-2} \text{s}^{-1}$ for 9 h, and then MR was measured. Dark-adapted tomato leaves were irradiated with far-red light (200 $\mu\text{mol m}^{-2} \text{s}^{-1}$). Dark reduction rates of P700⁺ were determined by switching off the far-red light after a 100 s irradiation. The decay signal was detected with a time of 12 s until the steady P700 photooxidation was got. The initial rate of P700⁺ re-reduction (0–0.3 s) was calculated as the rate of CEF (Wang et al. 2006). Three biological replicates were used in each genotype.

Determinations of H₂O₂ and O₂^{•-} levels, and antioxidant enzymes activities

The production rate of the superoxide anion (O₂^{•-}) was estimated as described by Elstner and Heupel (1976). Levels of H₂O₂ were tested as the method of Alia et al. (1999).

Ascorbate peroxidase (APX) and catalase (CAT) activities were estimated as described by Bartoli et al. (1999). Superoxide dismutase (SOD) activity was determined following the method described by Giannopotitis and Ries (1977). Peroxidase (POD) activity was measured according to the method of Maehly and Chance (2006), with one unit defined as an absorbance change of 0.1 units min⁻¹ at 470 nm. Enzyme activity assays were performed with a UV-visible spectrophotometer (UV-2550, Shimadzu, Kyoto, Japan). Five biological replicates were used in each genotype.

Thylakoid membrane preparation

The leaves of WT and L28 lines were taken in this experiment after low temperature (4 °C) treatment for 24 h. Thylakoid membranes were extracted as the method of Zhang et al. (1999). Tomato leaves were grinded in an ice-cold extraction buffer solution (50 mM HEPES pH 7.8, 400 mM sucrose, 10 mM NaCl, 2 mM EDTA, and 2 mM MgCl₂) on crushed ice and transferred to a new centrifuge tube. The mixture was centrifuged at 4200g for 5 min. The sediments were then washed with extraction buffer and centrifuged again. Thylakoid membrane pellets were suspended in isolation buffer and they were used fresh. The samples were from three independent plants for each genotype.

Detection of chlorophyll protein complexes by Blue Native PAGE (BN-PAGE)

BN-PAGE was performed according to standard methods (Schägger and von Jagow 1991). The thylakoid membranes were washed in an ice-cold isolation buffer (300 mM sorbitol, 5 mM MgCl₂, 20 mM HEPES-KOH and 2.5 mM EDTA, pH 7.0), and moved to a new ice-cold resuspension buffer (5 mM

MgCl₂, 2.5 mM EDTA and 20 mM HEPES-KOH, pH 7.0). And then, the same amounts of sample solubilization buffer containing 2% (w/v) DM was added to the thylakoid suspension. After incubated at 4 °C for 10 min, insoluble material was centrifuged at 20,000g for 10 min. The supernatant was combined with one-tenth volume of BN sample buffer [5% Serva blue G, 200 mM BisTris-HCl, pH 7.0, 1 M 6-amino-*n*-caproic acid, and 40% (w/v) glycerol]. After recentrifuged for 5 min, the supernatants were applied to 6 to 12% acrylamide gradient gels in a Hoefer Mighty Small vertical electrophoresis unit put in a transparent freezer (4 °C). The samples were from three independent plants for each genotype.

Total protein extraction and western blotting

The total protein was extracted from leaves of L28, WT+GB and WT tomato plants under normal conditions (25 °C), chilling stress (4 °C) for 5 days and recovery (25 °C) for 5 days. Fresh tomato leaves were pulverized in a chilled mortar with 1 mL of protein-extraction buffer (100 mM Tris-HCl, 1 mM EDTA-Na₂, 1% PVP, 10 mM β -mercaptoethanol, 0.4 mol L⁻¹ sucrose, pH 7.5). The mixture was then centrifuged at 12,000 g at 4 °C for 15 min. The supernatant was gathered as total protein of leaves and the concentrations were quantified using the dye-binding assay as the method described by Bradford (1976). Loading of samples was combined with Coomassie Brilliant Blue G-250 (BioRad) for staining of gels. All samples were boiled in a boiling bath for 1 min. For immune blotting, quantitative image analysis was conducted using a Tanon Digital Gel Imaging Analysis System (Tanon-4100; Shanghai Tanon Science & Technology Co, Ltd). Western blotting was performed with D1 antibody for blot analysis. The samples were from three independent plants for each genotype.

Statistical analyses

The data were preprocessed using Microsoft Excel 2010 (Microsoft, Redmond, WA), and SigmaPlot 12.5 (Systat Software, Erkrath, Germany) was used to generate the figures. Among the data, SAS (version 8.1; SAS Institute, Cary, NC) was used to determine the significant differences with an analysis of variance followed by Student's *t* test at $P < 0.05$ (*) or $P < 0.01$ (**) among the WT, WT+GB, and *BADH*-transgenic tomato plants. The mean values \pm standard error (SE) of at least three replicates are presented.

Results

Accumulation of GB, chlorophyll content, and growth in *BADH*-transformed young tomato seedlings

To investigate the beneficial physiological effect of GB on the growth of tomato seedlings under chilling stress, we measured the plant phenotype and fresh weight (Fig. 1). Although the growth of all tomato plants was inhibited after chilling stress, plants with applied GB and transgenic plants grew better than did WT plants (Fig. 1a, c). As shown in Table S1, the GB levels of tomato leaves in the *BADH*-transgenic lines (Lines 10 and 28) and WT plants applied with 5 mM GB (WT + GB) ranged from 2.9 $\mu\text{mol g}^{-1}$ fresh weight to 6.7 $\mu\text{mol g}^{-1}$ fresh weight, while GB was almost undetectable in leaves of WT plants. Besides, the endogenous level of GB in chloroplasts of *BADH*-transgenic plants was six to tenfold higher than in WT + GB plants. All GB-accumulated plants recovered and grew faster than WT plants after chilling stress treatment for 5 days.

To understand the change in light absorption, we detected the levels of chlorophyll (Chl). There were no obvious differences observed among all lines in Chl contents under normal conditions. However, under chilling stress, Chl content decreased in all seedlings, but Chl in *BADH*-transgenic and GB-treated WT plants maintained higher levels compared with that of the WT. Besides, when seedlings were transferred to normal conditions for recovery, Chl content continued to decrease sharply (Fig. 1b), but transgenic lines and WT + GB plants still maintained a higher content of chlorophyll.

Chloroplast structure and photosynthetic responses to chilling in WT and transgenic lines

At room temperature (25 °C), chloroplasts in Line 28 and the WT were arranged in a spindle shape adjacent to the cell membrane along the cell wall, while chloroplasts and starch grains of Line 28 were larger than those in the WT. The chloroplast grana lamella of the two tomato lines were arranged neatly and the cell membrane and chloroplast envelope were intact. After 5 days of chilling treatment, chloroplasts in the WT were vertically arranged with cell

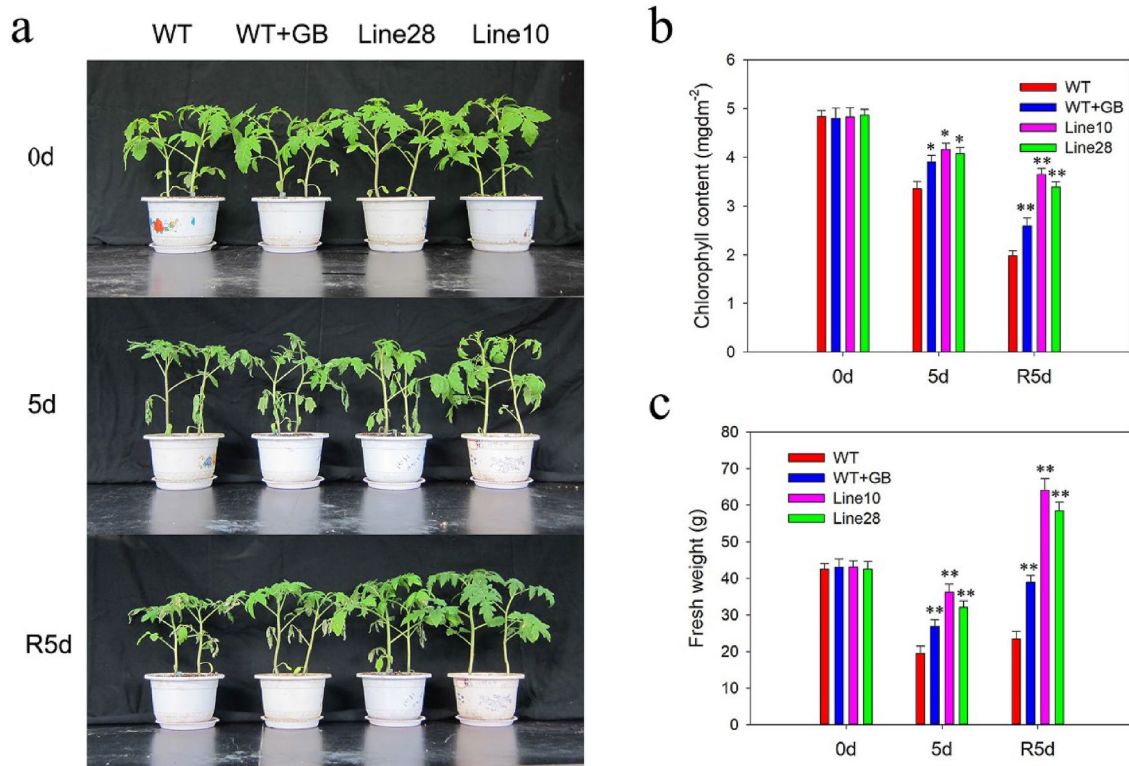


Fig. 1 Growth analysis of tomato plants at room temperature (25 °C), low temperature (4 °C), and recovery (25 °C) for 5 days. **a** Phenotype of the grown plants. **b** The content of total chlorophyll in tomato seedlings. **c** Fresh weight of tomato seedlings. Tomato plants growing under normal conditions were exposed to low-temperature conditions

for 5 days and then placed under normal conditions for another 5 days for recovery. The values are means \pm standard error (SE) ($n=3$). ** and * indicate that the differences between various strains were significant at 0.01 and 0.05, respectively

walls, whereas chloroplasts in Line 28 were not (Fig. S1). This arrangement helped to reduce the absorption of light energy by the WT. Furthermore, most of the grana lamella of the WT chloroplasts were destroyed, whereas only part of the grana lamella of Line 28 chloroplasts was destroyed under chilling stress. It was obvious that GB *in vivo* could protect the grana structure of chloroplasts and conferred strong chilling tolerance for tomato plants.

For further evaluation of the differences in photosynthesis among the WT, *BADH*-transgenic, and WT+GB tomato seedlings in response to chilling stress, CO₂-exchange parameters were measured. Under normal temperature conditions, there were no significant differences among the WT, WT+GB, and *BADH*-transgenic tomato seedlings in any parameters (Fig. 2). However, during the following 5 days chilling period, although photosynthetic rate (P_n) declined in the WT, transgenic lines, and WT+GB, a much faster rate of decline was exhibited by the former (Fig. 2). When the plants were exposed to normal conditions for recovery, P_n of all plants increased again, and P_n of transgenic lines and WT+GB increased more quickly than did that of the WT seedlings. Similar changes were also observed in the stomatal conductance (G_s) and the transpiration rate (T_r). Chilling caused evident increases in intercellular CO₂ concentration (C_i) in

all plants, but the C_i in WT was much higher than that in the *BADH*-transgenic lines and WT+GB plants.

GB biosynthesis alleviated PSII photoinhibition induced by chilling stress

To investigate the effect of GB on PSII photoinhibition, maximal photochemical efficiency (F_v/F_m), electron transport rate (ETR) and photochemical quenching (q_p) were determined. Under normal conditions, F_v/F_m , q_p , and ETR showed no significant difference among the all tomato plants. However, under chilling stress, although the values of F_v/F_m , q_p , and ETR decreased in all types of tomato leaves, they decreased much more sharply in the WT plants than in the other lines when exposed to chilling stress. After 5 days for recovery, F_v/F_m , q_p , and ETR of *BADH* transgenic and GB-treated WT plants recovered more rapidly than did that of the WT plants (Fig. 3a–c).

Moreover, $(1 - q_p)/NPQ$ represents the excess excitation energy of the PSII reaction center, then $(1 - q_p)/NPQ$ and the relationship between F_v/F_m and $1 - q_p$ (PSII excitation pressure) were analyzed. After chilling stress, $(1 - q_p)/NPQ$ gradually increased, and $(1 - q_p)/NPQ$ of transgenic lines (line 10, line 28) increased slightly, whereas that of the WT increased substantially (Fig. 3d). Plants exposed to low

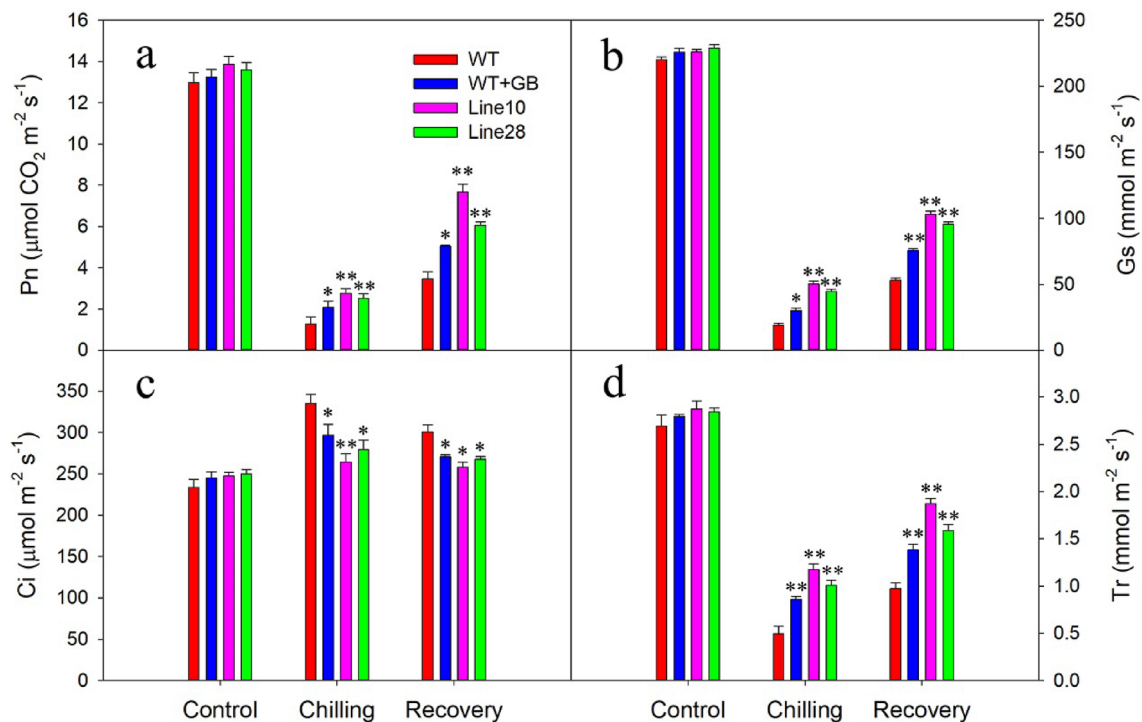


Fig. 2 Changes of P_n (a), G_s (b), C_i (c), and T_r (d) in tomato leaves of the WT, *BADH*-transgenic tomatoes, and WT+GB plants. Seedlings grown at 25 °C were transferred to 4 °C in chambers for 5 days and then they were exposed to 25 °C for recovery for approximately

5 days. The values are means \pm SE ($n=3$). * and ** indicate that the differences between various strains are significant at 0.05 and 0.01, respectively

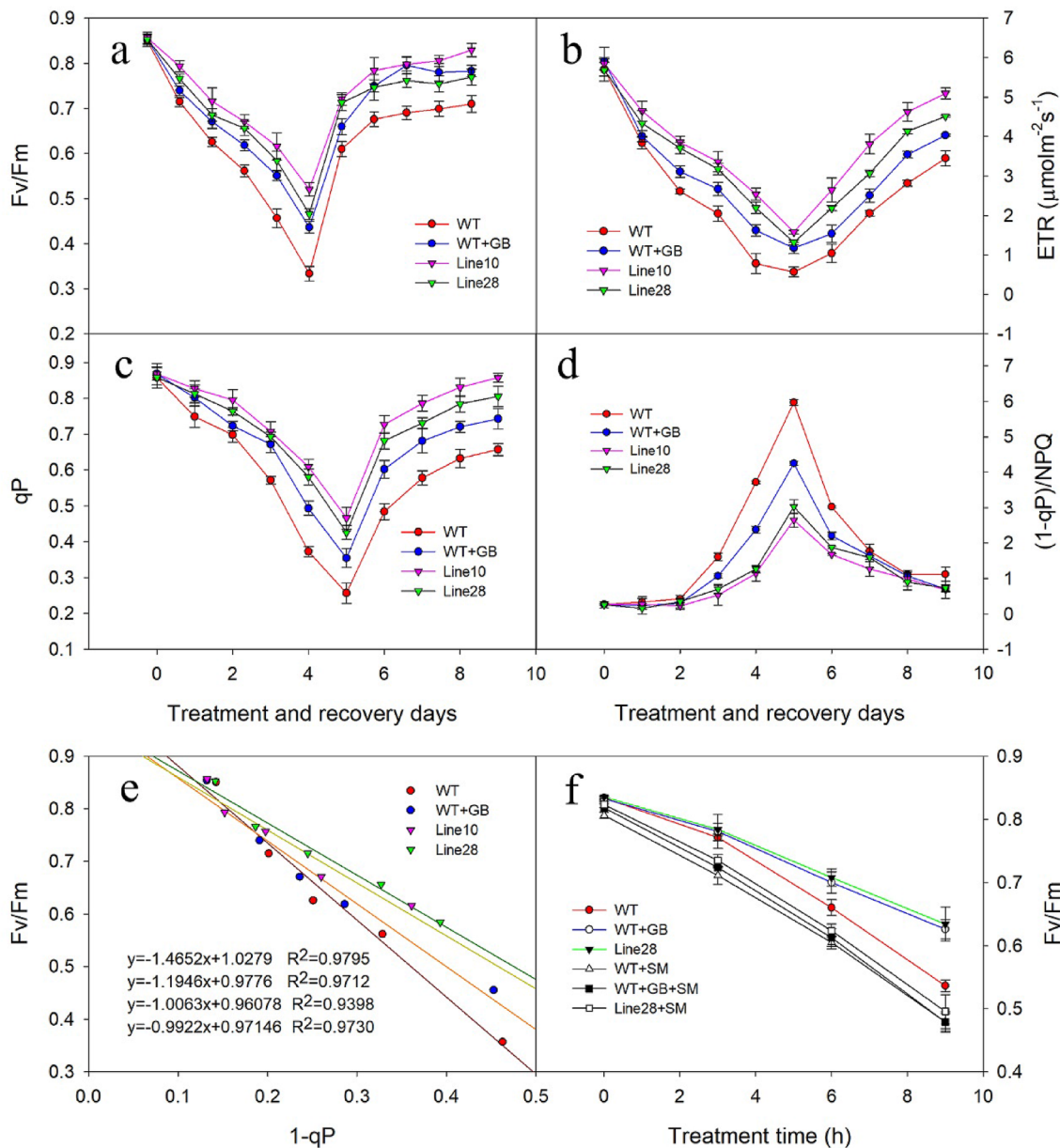


Fig. 3 Changes in F_v/F_m , ETR, q_p , and $(1-q_p)/NPQ$ in WT, WT+GB, and *BADH*-transgenic tomato seedlings under chilling stress. **a** The maximum quantum yield of PSII, F_v/F_m . **b** Electron transport rate, ETR. **c** The ratio of open reaction centers, q_p . **d** Excitation energy, $(1-q_p)/NPQ$. Tomato plants were transferred to 4 °C in an incubator for 5 days and then placed into normal conditions for

5 days of recovery. **e** Relationships between PSII excitation pressure ($1-q_p$) and F_v/F_m in tomato leaves. Tomato plants were growing at normal temperature (25 °C), then exposed to 4 °C in an incubator for 5 days. **f** Changes of F_v/F_m in isolated function leaves of WT, WT+GB, and *BADH*-transgenic plants under chilling and SM treatment for 9 h. The values are means \pm SE ($n=3$)

temperatures may induce high excitation pressure, which results in an energy imbalance. As shown in Fig. 3e, the values of PSII excitation pressure ($1-q_p$) increased with the decrease of F_v/F_m , there were no significant differences in those slopes of transgenic leaves. However, with the increase of $1-q_p$ and F_v/F_m of the WT declined much more sharply than did that of transgenic lines and GB-treated plants. These results demonstrated that the lower PSII photoinhibition in

transgenic lines and GB-treated plants are likely associated with the lower PSII excitation pressure.

Furthermore, as shown in Figure S2, we also used diuron (DCMU) to block the electron transporting from Q_A to Q_B in the thylakoid membrane. F_v/F_m in all tomato leaves was declined under chilling stress and DCMU treatment. F_v/F_m of GB accumulated lines was much higher than that of WT plants. It means that in addition electron transport,

the protection mechanism of GB on PSII may be associated with other pathways.

To confirm whether the protective effect of GB on PSII may be related to the de novo synthesis of the D1 protein, we used streptomycin sulfate (SM), an inhibitor of the de novo synthesis of the D1 protein, treatment on tomato plants. Compared with WT, F_v/F_m maintained higher levels in WT+GB and Line 28. After chilling treatment for 9 h, F_v/F_m decreased by approximately 35.7%, 24.8%, and 24.1%, respectively, in WT, WT+GB, and Line 28, compared to that of the control (Fig. 3f). With SM treatment, F_v/F_m decreased by approximately 47.9% in the three tomato lines compared to that of the control. Furthermore, F_v/F_m of the lines with SM treatment was lower than that without SM treatment (Fig. 3f). Thus, the protective effect of GB on PSII may be dependent on the de novo synthesis of D1 protein.

OJIP curve, JIP test parameters, and energy distribution models

As shown in Fig. 4a, chlorophyll fluorescence curves from all treatments displayed typical chlorophyll fluorescence transient (OJIP) transients when plotted on a logarithmic time scale. No evident changes in OJIP curves were observed in all lines under normal conditions. However,

the fluorescence rise slowed and reached a much lower “P” level in lines suffered from chilling stress for 5 days and that of the WT decreased more significantly.

A “spider plot” showed the values of most parameters characterizing PSII function. In the “spider plot” diagram, pronounced changes were observed in many of the estimated parameters in the lines after 5 days chilling treatment compared to normal growth plants (Fig. 4b). The values of several parameters: ϕ_{Eo} (quantum yield for electron transport), ϕ_{Po} (the maximum yield of primary photochemistry of PSII), Ψ_o (the exciton efficiency of electron transport beyond Q_A^-), and PI_{ABS} (the performance index) decreased in all tomato plants after chilling treatment, whereas these parameters in transgenic lines and WT+GB were higher than those in the WT plants. Furthermore, the fraction of the primary quinone electron acceptor of PSII, V_j , increased in the WT, transgenic lines, and WT+GB at a much slower rate for the former under chilling stress. Interestingly, the values of S_m (multiple turnovers of Q_A reduction events) and N (the number of Q_A redox turnover before F_m is reached) in transgenic lines and WT+GB increased when plants were exposed to low temperature, whereas that of the WT decreased when suffering from chilling stress. These data indicated that GB-accumulated in vivo and in vitro alleviated the decline of efficiency of

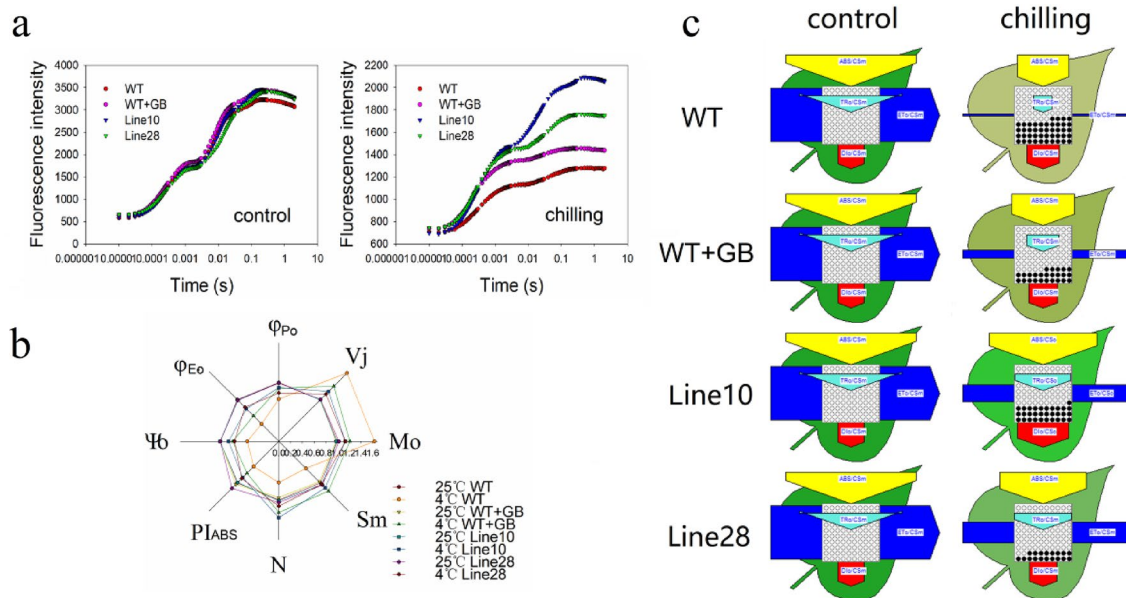


Fig. 4 The changes of chlorophyll fluorescence and JIP test. **a** Chlorophyll *a* fluorescence transient (OJIP) curves of tomato seedlings of WT, WT+GB, and transgenic lines (line 10, line 28) under normal conditions (25 °C) and chilling stress at 4 °C for 5 days. **b** A “spider diagram” of selected fluorescence parameters characterizing PSII behavior of tomato leaves exposed to 5 days of chilling stress (for the meaning of the symbols and parameters, please refer to the table of Nomenclature). All the values are shown as percent of control (con-

rol plants=5). **c** The phenomenological leaf model is used to compare the differences among the control, chilling stress and recovery. Each arrow thickness represents the values of electron transport flux (ET_o/CS_m), absorbance (ABS/CS_m), heat dissipation of excess light (DI_o/CS_m) and trapping energy flux (TR_o/CS_m); all expressed per leaf CS. In leaf models, the open circles and closed circles represent the active and inactive RCs, respectively

electrons into the electron transport chain (ETC) under chilling stress.

In order to directly visualize and more insight into the changes in photosynthetic apparatus caused by chilling stress, energy pipeline models of phenomenological fluxes per excited CS (CS_m) after chilling stress treatment for 5 days in the tomato leaves were constructed (Fig. 4c). The fraction of inactive reaction centers was represented by the black points. WT plants had a much lower ET_o/CS_m (electron transport flux per CS) than normal growth plants and the number of nonactive reaction centers increased when plants were treated with chilling stress for 5 days. Moreover, the chilling-stressed transgenic lines had much higher DI_o/CS_m (dissipation per CS) than did the normal growth plants. TR_o/CS_m (maximum trapping flux beyond Q_A per CS) displayed a similar tendency as ET_o/CS_m (Fig. 4c).

P700 oxidoreduction and the rate of CEF under chilling stress

To further characterize PSI electron transport capacity and CEF around PSI under chilling stress, we performed 820 nm absorbance measurements on leaves of tomato plants. According to the maximal slopes of P700 absorption change kinetics curve, we can calculate the P700 oxidation and the following re-reduction rates (Fig. 5a). The photooxidation effect of illumination on P700 is usually used as an important indicator of PSI electron transport capacity. P700 oxidation rate (V_{ox}) decreased following chilling treatment and it dropped more severely in the WT tomato plants than in *BADH*-transgenic and WT+GB tomato plants. After 5 days of recovery at 25 °C, the P700 oxidation rate continued to decrease and the decline was more serious in WT seedlings (Fig. 5a), indicating a higher PSI electron transport capacity in *BADH*-transgenic and WT+GB plants. When tomato

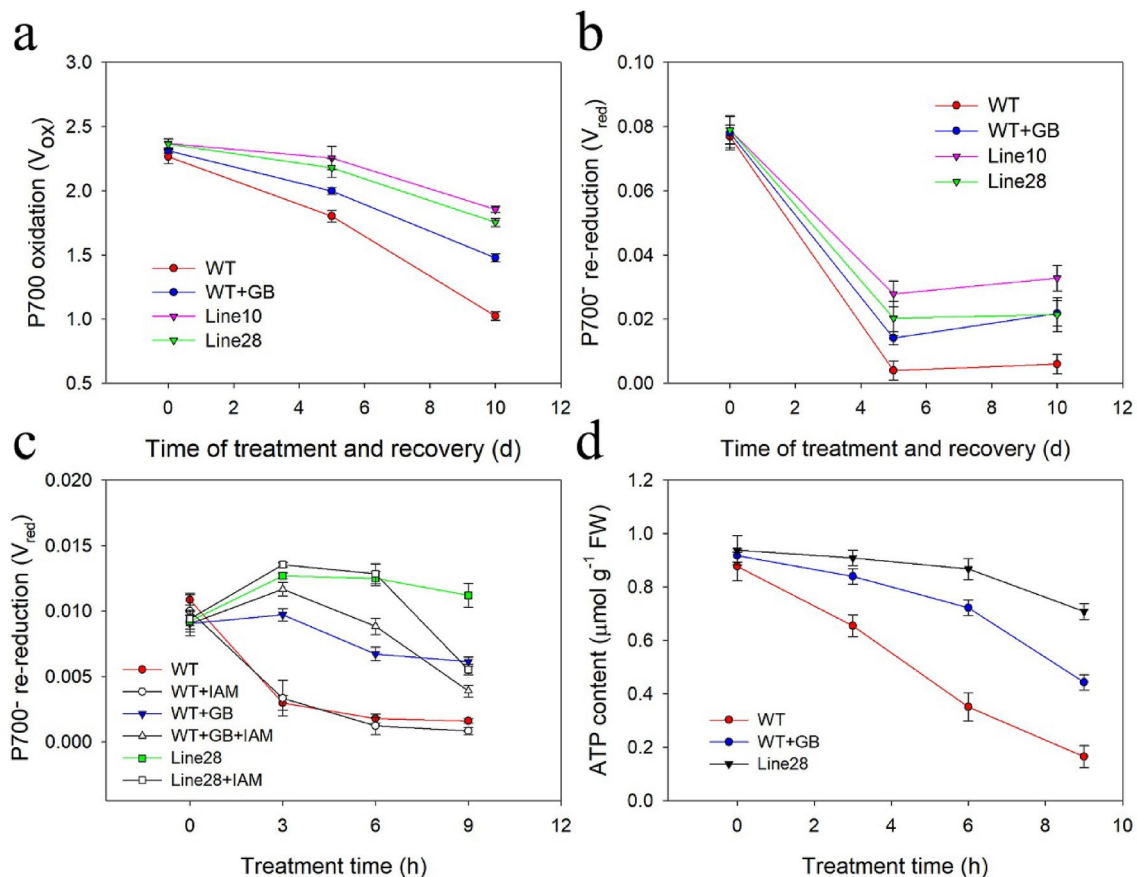


Fig. 5 Analysis of P700 by 820 nm transmission and ATP content. **a** In a fully expanded leaf of the WT and *BADH*-transgenic lines, the rate of P700 oxidation of kinetics of modulated 820 nm reflection was detected by M-PEA when tomato plants were treated at 4 °C for 5 days and 25 °C for recovery over the next 5 days. **b** Changes in the initial rates (0–0.3 s) of P700⁺ re-reduction following far-red light in tomato leaves transferred to 4 °C for 5 days, subsequently at

25 °C in WT, WT+GB, and transgenic lines. **c** Changes in the initial rates (0–0.3 s) of P700⁺ re-reduction following far-red light in isolated tomato leaves with and without 0.02 mM iodoacetamide (IAM) for 9 h under chilling stress in the WT, WT+GB, and Line 28. **d** Changes of ATP content after chilling stress for 9 h in tomato leaves. The values are means \pm SE ($n=3$)

plants were exposed to 4 °C chilling treatment, we observed that the P700⁺ re-reduction rate was more greatly affected than that of P700 oxidation.

The dark re-reduction of P700⁺ could reflect the rate of cyclic electron transport (CET) around PSI. The dark re-reduction of P700⁺ decreased during chilling stress (Fig. 5b), which was revealed when the rate of CET around PSI was suppressed by the chilling treatment. However, the CET rate was higher in *BADH*-transgenic lines than that of the WT plants. During the recovery process, the rate of CET around PSI in transgenic line leaves increased faster than did that in the leaves of the WT.

To understand the response of CEF on chilling without electron receptors in the Calvin cycle, we used iodoacetamide (IAM), an inhibitor of blocking the Calvin cycle. With the presence of IAM, the rate of CET in leaves was lower than that of plants without IAM at first. When isolated tomato leaves were placed in low-temperature conditions, the rate of CET was stimulated at first in transgenic plants Line 28 and WT + GB, then decreased during 9 h of chilling treatment. However, the rate of CET in the WT plants continually decreased until reaching a low level at 9 h (Fig. 5c). The results showed that the CET was strengthened after the Calvin cycle was inhibited in GB-accumulated plants, and this aided in consuming extra electrons from the photosystems under chilling stress.

Under normal conditions, the content of ATP in GB-accumulated and control plants was approximately the same (Fig. 5d). ATP content decreased after chilling stress for 9 h in all tomato plants but it was significantly lower in the WT plants, indicating that GB alleviated ATP consumption under chilling stress.

Changes of PSII and PSI protein contents under chilling stress

The total protein was extracted from the fully extended tomato leaves exposed to 4 °C and low irradiance for 5 days. The protein gel blot analysis showed no significant variation in the D1 levels among WT, WT + GB, and transgenic lines under control conditions (Fig. 6a). Although the levels of D1 protein in all genotypes decreased markedly, the decline in the WT was more serious than that in the *BADH*-transgenic lines after chilling stress.

The activity of PSII and the levels of D1 protein were affected by chilling stress (Figs. 3a, 6a). Therefore, we next performed a BN-PAGE analysis to test the contents of PSII protein complexes and other photosynthetic membrane protein in WT and Line 28. Five major bands labeled I–V were resolved, apparently representing PSII–LHCII super complexes (band I), monomeric PSI, dimeric PSII (band II), monomeric PSII (band III), CP43-free PSII (band IV), trimeric LHCII/PSII reaction center (band V), and unassembled

proteins (band VI). Few differences were apparent in the BN gel, except the amount of PSII–LHCII super complexes (band I), which was slightly more in Line 28 than in the WT plants after chilling for 5 days. The amount of PSII–LHCII super complexes (band I), monomeric PSI, and dimeric PSII (band II) of the two lines decreased more significantly in the WT than in Line 28 (Fig. 6b, c). Our results demonstrated that GB was able to maintain the thylakoid protein complex stability, thereby increasing chilling tolerance.

GB alleviated the oxidative stress induced by chilling stress

When the balance of electrons from PSII to PSI was broken, electrons were transferred to O₂ and then ROS were produced. In turn, ROS attacked plasma membranes and proteins in the photosystem. In our study, we detected levels of H₂O₂ and the production rate of O₂^{•−}. Under normal conditions, H₂O₂ accumulated at low levels and appeared similar in the WT, WT + GB lines, and *BADH*-transgenic tomato plants (Fig. S3). However, H₂O₂ levels and O₂^{•−} production rate increased under chilling stress even during subsequent recovery treatment. Furthermore, there were more ROS generated in the WT plants than in transgenic lines and the WT + GB plants, which indicated that GB could mitigate the oxidative stress induced by chilling stress.

Furthermore, APX activity increased under chilling stress and this increase was slower in WT plants compared to that of *BADH*-transgenic tomato plants. The SOD activity increased after 3 days of chilling treatment and then decreased following additional days of treatment (Fig. S3). The enhanced antioxidant enzymes (APX, SOD, CAT, and POD) activities in *BADH*-transgenic lines and WT + GB reduced H₂O₂ and O₂^{•−} accumulation.

Discussion

GB accumulation in vivo and in vitro could shield plants against chilling stress (Park et al. 2004, 2006; Farooq et al. 2008). However, the physiological and molecular mechanisms of how GB confers chilling tolerance to plants by protecting the photosynthetic machinery remained to be further elucidated. In our study, GB from genetic engineering synthesis and foliar application alleviated chilling-induced growth inhibition (Fig. 1a). Despite the substantial reductions in photosynthetic capacity caused by chilling, the accumulation of GB in tomato leaves alleviated this change, that is, the transgenic and WT + GB plants still maintained the higher Pn under chilling stress, as well as had the stronger resilience (Fig. 2). Furthermore, under chilling stress the results of microscopy showed that GB can protect the structure of chloroplasts in tomato leaves in vivo (Fig. S1), which may be related to the ability of transgenic lines to maintain

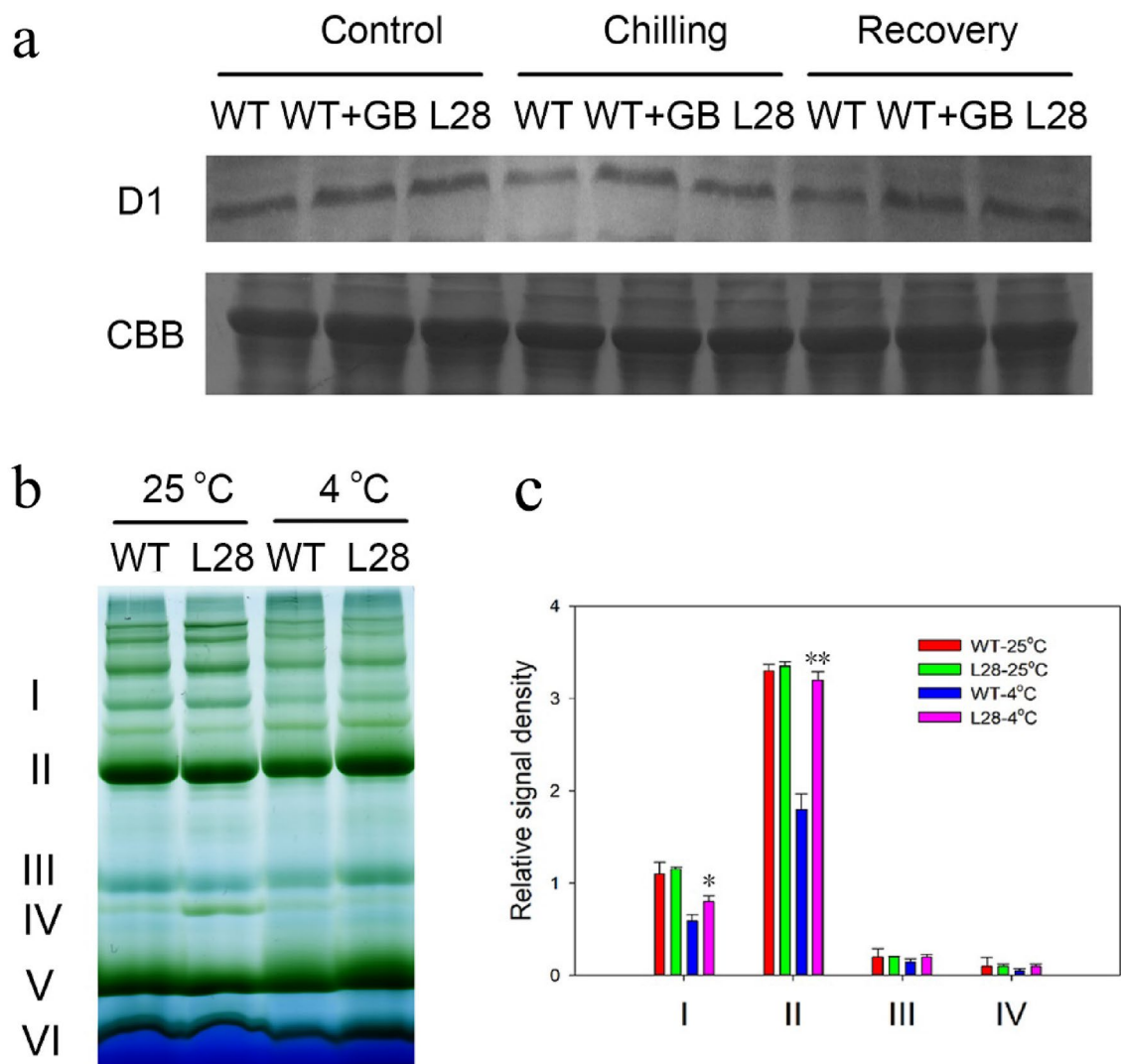


Fig. 6 Analysis of D1 by western blotting and stability of thylakoid membrane complexes analyzed by BN-PAGE. **a** The levels of D1 protein in tomato leaves of WT, WT+GB, and line 28 were treated under normal (25 °C), chilling (4 °C) and recovery (25 °C) for 5 days. Blots were stained with Coomassie Brilliant Blue (CBB) G-250 (BioRad). **b** The effects of GB on PSII cofactor–protein complexes in tomato leaves under chilling stress. Thylakoid membranes of BN-PAGE separation in the WT and Line 28 were treated under normal

(25 °C) and chilling stress (4 °C) for 24 h, six separated protein complexes are indicated on the right. **c** Quantitative image analysis of protein levels in **b** using a Tanon Digital Gel Imaging Analysis System. The relative proteins in the *BADH*-transgenic tomato plants were normalized to the level of LHCII complex (band I) in the WT under the control. The data are shown as means \pm SD. * and ** indicate that differences between various stains are significant at 0.05 and 0.01, respectively

strong chilling resistance, thereby contributes to the orderly operation of photosynthesis under low temperature stress.

Most of the sunlight energy absorbed in the photosynthetic apparatus is directed towards photochemistry and ETR (Baker 2008; Tadmor et al 2021). In our experiment, the transfer of the *BADH* gene into tomatoes also relieved PSII photoinhibition (Fig. 3a). Photoinhibition may be caused by the inactivation of reaction center and a decrease in the electron transport rate under chilling stress (Fig. 3b). Additionally, over excitation of PSII can result in the formation of ROS, photodamage, and ultimately inactivation of PSII

(photoinhibition) (Derks et al. 2015; Derks and Bruce 2018; Bednařiková et al. 2020). Interestingly, under chilling stress, the PSII excitation pressure ($1 - q_p$) was lower in GB-accumulated plants such that $(1 - q_p)/NPQ$ (the excess excitation energy of PSII reaction center) was significantly lower in GB-accumulated plants than that in the WT (Fig. 3d, e). Furthermore, F_v/F_m of the tomato plants with SM treatment was significantly lower than that without SM treatment (Fig. 3f), suggesting that the protective effect of GB on PSII may be dependent on the de novo synthesis of D1 protein (Ohnishi and Murata 2006; Li et al. 2021b). Therefore, the possible

mechanism by which GB protects the PSII reaction centers against chilling stress is the reduction of PSII excitation pressure (Fig. 3c, d, e) and the repair of the PSII protein (Fig. 3f).

The ultimate regulator of the photosynthetic electron transfer chain is the modulation of PSII inhibition, which provides a photoprotective mechanism against the formation of ROS and photodamage in PSI (Tikkanen et al. 2014). Thylakoid linear electron transport (LET) was limited by chilling stress because of increased oxidative stress induced by light (Allen and Ort 2001). The OJIP fluorescence transient shape is extremely sensitive to various types of abiotic stresses (Strauss et al. 2006; Perreault et al. 2011; Bednařková et al. 2020). In this study, the curves of OJIP changed rapidly under chilling stress in tomato plants and the PSII ETC was more substantially influenced in the WT than the GB-accumulated plants by chilling stress (Fig. 4a). Chlorophyll *a* transient kinetics analysis showed that more electrons were transferred into the linear electron chains (Ψ_o) in GB-accumulated plants (Fig. 4c). Furthermore, in PSII and PSI, the energy of the harvested photons induces charge separation. Electrons from the PSII primary donor P680 pass via pheophytin and the primary quinone Q_A to the secondary quinone, Q_B (Solymosi et al. 2020). Although the redox reaction after Q_A (ϕ_{P_0}) was inhibited by chilling stress and resulted in the slowing of the electron transfer between Q_A^- and Q_B (V_j), GB mitigated this inhibition (Fig. 4c). Furthermore, diuron (DCMU) can block the electron transporting from Q_A to Q_B in the thylakoid membrane (Guo et al. 2020). From our results, F_v/F_m of GB accumulated lines was much higher than that of WT plants with chilling and DCMU treatments (Fig. S2). Thus, GB has an important effect on the process of electron transfer from Q_A to Q_B . Moreover, more energy was used for heat dissipation (ϕ_{D_0}), and more excess excitation energy occurred in the WT tomato plants than that in *BADH* tomato plants (Fig. 4b, c). The PSII ETCs was more tolerant of low temperatures in the *BADH*-transgenic tomato leaves than that in WT tomato leaves, which is one of the reasons why a higher Pn was maintained in the GB-accumulated plants under chilling stress.

As PSI and PSII work in series, a balanced excitation distribution between the two photosystems is required for optimal photosynthetic efficiency (Joliot and Johnson 2011; Lima-Melo et al. 2019). It is required for CEF around PSI to generate a proton gradient that, in turn, leads to the efficient NPQ in *Ficus concinna* trees under heat stress (Jin et al. 2009). GB can alleviate the decrease of PSI electron transport capacity and the rate of CEF in vivo and in vitro (Fig. 5a, b). According to the reports, the content of chlorophyll is closely associated with the activity of PSI, which indicates that a decrease in the amount of chlorophyll could be caused by the degradation of the PSI reaction center

complex (Kudoh and Sonoike, 2002; Montepietra et al. 2020). In our research, the effect of GB on protection of chlorophyll may have a positive effect on the PSI electron transport capacity during chilling and recovery (Fig. 5a). When chilling limited CO₂ photosynthetic fixation, excitation pressure was enhanced because of the accumulation of excess reductants on the PSI acceptor side, thereby causing the balance between PSII and PSI to be destroyed (Roach and Krieger-Liszkay 2014). Afterward, CET was stimulated rapidly. In our study, the rate of CEF was enhanced more significantly in GB-accumulated tomato plants than that in the WT (Fig. 5b). Because IAM was used in this study, the rate of CEF was stimulated in transgenic lines and WT + GB, which indicated that GB affected CEF (Fig. 5c). Moreover, CEF may be triggered by a reduction of PQ pool mediated either by an imbalance between nonphotochemical reduction and oxidation PQs or by PSII activity (Thierry et al. 2002). The increase in the turnover number of Q_A (S_m) may be associated with the increase of CEF in tomato plants accumulating GB (Figs. 4c, 5c). Therefore, GB affected CEF and the increasing rate of CEF may contribute to the reduction of excitation pressure.

Moreover, one possible function of the CET around PSI is to synthesize the extra ATP to adjust the ratio of NADPH to ATP (Johnson 2011; Huang et al. 2018). Takahashi et al. (2009) proposed that the photosynthetic CEF can protect plants from the inhibition of PSII by both preventing PSII photodamage and minimizing the inhibition of the repair of the damaged PSII. The rate of PSII repair was reduced upon inhibition of the synthesis of ATP either via PSI or PSII, indicating that the rapid repair of photodamaged PSII complexes (such as D1 protein) requires a large amount of ATP in a short time (Allakhverdiev et al. 2005; Murata et al. 2007; Murata and Nishiyama 2018). Thus, a higher level of ATP in GB-accumulated plants may play a significant role in D1 repair (Fig. 5d). In addition, the western blot and BN-PAGE analysis demonstrated that the contents of PSII–LHCII super complexes, monomeric PSI, dimeric PSII and D1 protein declined more in the WT tomato plants than that in transgenic lines under chilling stress (Fig. 6). Consequently, the enhanced rate of CEF by GB could provide positive effects in the production of more ATP for the repair of PSII complexes, thereby maintaining the thylakoid protein complex stability under chilling stress (Figs. 3f, 5c, d, 6).

ROS are mainly generated in chloroplasts and formed both on the electron donor side of PSII and the electron acceptor side of PSI during light reactions (Roach and Krieger-Liszkay 2014; Sasi et al. 2018). The superoxide anion radical or singlet oxygen (O_2^-) will be produced when more electrons are released in the ETC than the electron-consuming capacity of Calvin cycle (Nishiyama and Murata 2014). As in our study, transferring a spinach *BADH* gene from spinach to tomato plants causes a GB biosynthesis

process that may have an active effect by consuming electrons in the ETCs. In WT plants, more electrons were allocated to dioxygen (O_2). Thus, more ROS are produced (Fig. S3a, b). H_2O_2 can seriously destroy the activity of PSI on thylakoid membranes under light (Sonoike et al. 1997). Studies have shown that ROS generated by H_2O_2 and square one iron–sulfur clusters can damage PSI under low light and chilling stress (Ogawa et al. 1997). GB activated the activities of antioxidant enzymes to eliminate ROS (Fig. S3c, d, e, f), which may contribute to the protection of PSI.

Taken together, we proposed a model of GB on photosynthetic systems in tomato under chilling stress (Fig. 7). When tomato plants were transferred from optimal temperature to low temperature, excess excitation energy increased and induced ROS generation, resulting in the photoinhibition of PSII and PSI, whereas either GB accumulated in vivo in *BADH*-transgenic tomato plants or GB applied in vitro can improve chilling tolerance by protecting chloroplast ultrastructure and alleviating photosystem photoinhibition under long-term chilling stress. On the other hand, GB stimulated the rate of CEF to consume extra electrons in the electron transport chain during chilling and recovery, as to decrease the accumulation of excess reductants at the acceptors of PSI and transfer fewer electrons to O_2 , scilicet, preventing an additional sink for the consumption of photosynthetically generated electrons and less ROS production. Moreover, GB also increased ATP content and antioxidant enzyme activity, accelerated D1 protein repair,

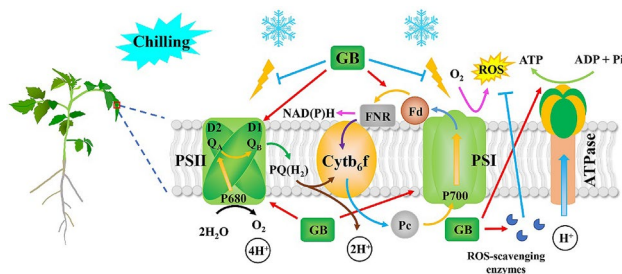


Fig. 7 Proposed mechanisms of GB protection on photosystems in tomato leaves under low-temperature stress. Chilling stress could cause the increase of excess excitation energy, which induces ROS generation, resulting in the photoinhibition of PSII and PSI, whereas either GB accumulated in vivo or in vitro improve chilling tolerance by protecting chloroplast ultrastructure and alleviating photosystems photoinhibition under long-term chilling stress. On the other hand, GB stimulated the rate of CEF in consuming extra electrons in the ETC during chilling and recovery to decrease the accumulation of excess reductants at the acceptors of PSI and transfer fewer electrons to O_2 , scilicet, preventing an additional sink for the consumption of photosynthetically generated electrons and less ROS production. Moreover, GB could increase ATP content and antioxidant enzyme activity, accelerate D1 protein repair, and maintain photosystem stability, finally enhancing chilling tolerance of photosystems I and II in *BADH* transgenic and GB-treated tomato plants under chilling stress. *FNR* Fd: NADP⁺ oxidoreductase, *PC* plastocyanin

and maintained photosystem stability. Finally, it enhanced chilling tolerance of PSI and PSII in *BADH*-transgenic and GB-treated tomato plants under chilling stress.

Supplementary Information The online version contains supplementary material available at <https://doi.org/10.1007/s00299-022-02839-0>.

Author contributions statement XY conceived and supervised the project, and XY, YL and DW designed the experiments. DW and TZ performed most of the experiments. BW, HZ, MM and SL performed some of the experiments. DW, TZ and XY analyzed data and wrote the manuscript. THHC, MB and YL gave positive suggestion about this article. All authors read and approved the manuscript.

Funding Funding for this research were provided by the National Natural Sciences Foundation of China (31870216, 31470341), Open project of State Key Laboratory of Crop Biology of Shandong Agriculture University (2017KF10) and Science and Technology Innovation Project of Colleges and Universities in Shanxi Province (2020L0542).

Declarations

Conflict of interest The authors have no conflicts of interest to declare.

References

- Alia KY, Sakamoto A, Nonaka H, Hayashi H, Saradhi PP, Chen THH, Murata N (1999) Enhanced tolerance to light stress of transgenic *Arabidopsis* plants that express the *codA* gene for a bacterial choline oxidase. *Plant Mol Biol* 40:279–288
- Allakhverdiev SI, Nishiyama Y, Takahashi S, Miyairi S, Suzuki I, Murata N (2005) Systematic analysis of the relation of electron transport and ATP synthesis to the photodamage and repair of photosystem II in *Synechocystis*. *Plant Physiol* 137:263–273
- Allen DJ, Ort DR (2001) Impacts of chilling temperatures on photosynthesis in warm-climate plants. *Trends Plant Sci* 6:36–42
- Baker NR (2008) chlorophyll fluorescence: a probe of photosynthesis in vivo. *Annu Rev Plant Biol* 59:89–113
- Bartoli CG, Simontacchi M, Tambussi E, Beltrano J, Montaldi E, Puntarulo S (1999) Drought and watering-dependent oxidative stress: effect on antioxidant content in *Triticum aestivum* L. leaves. *J Exp Bot* 50:375–383
- Bednaříková M, Václav P, Lazár D, Barták M (2020) Photosynthetic performance of Antarctic lichen *Dermatocarpon polyphyllum* when affected by desiccation and low temperatures. *Photosynth Res* 145:159–177
- Bradford MM (1976) A rapid and sensitive method for the quantitation of microgram quantities of protein utilizing the principle of protein-dye binding. *Anal Biochem* 72:248–254
- Chen THH, Murata N (2002) Enhancement of tolerance of abiotic stress by metabolic engineering of betaines and other compatible solutes. *Curr Opin Plant Biol* 5:250–257
- Chen THH, Murata N (2008) Glycinebetaine: an effective protectant against abiotic stress in plants. *Trends Plant Sci* 13:499–505
- Chen THH, Murata N (2011) Glycinebetaine protects plants against abiotic stress: mechanisms and biotechnological applications. *Plant Cell Environ* 34:1–20
- Croce R, van Amerongen H (2020) Light harvesting in oxygenic photosynthesis: structural biology meets spectroscopy. *Science* 369:eaay2058

- Derks AK, Bruce D (2018) Rapid regulation of excitation energy in two pennate diatoms from contrasting light climates. *Photosynth Res* 1382:149–165
- Derks A, Schaven K, Bruce D (2015) Diverse mechanisms for photoprotection in photosynthesis. Dynamic regulation of photosystem II excitation in response to rapid environmental change. *BBA Bioenerget* 1847:468–485
- Ding YL, Shi YT, Yang SH (2020) Molecular regulation of plant responses to environmental temperatures. *Mol Plant* 13:544–564
- Elstner EF, Heupel A (1976) Inhibition of nitrite formation from hydroxylammoniumchloride: a simple assay for superoxide dismutase. *Anal Biochem* 70:616–620
- Farooq M, Aziz T, Hussain M, Rehman HU, Jabran K, Khan MB (2008) glycinebetaine improves chilling tolerance in hybrid maize. *J Agron Crop Sci* 1942:152–160
- Giannopoulou CN, Ries SK (1977) Superoxide dismutase in higher plants. *Plant Physiol* 59:309–314
- Gong ZZ, Xiong LM, Shi HZ, Yang SH, Herrera-Estrella LR, Xu GH, Chao DY, Li JR, Wang PY, Guo Y, Zhu JK (2020) Plant abiotic stress response and nutrient use efficiency. *Sci China Life Sci* 63:635–674
- Guo YJ, Lu YP, Goltsev V, Strasser RJ, Kalaji HM, Wang H, Wang XX, Chen SG, Qiang S (2020) Comparative effect of tenuazonic acid, diuron, bentazone, dibromothymoquinone and methyl viologen on the kinetics of Chl a fluorescence rise OJIP and the MR820 signal. *Plant Physiol Biochem* 156:39–48
- Huang W, Yang YJ, Zhang SB, Liu T (2018) Cyclic electron flow around photosystem I promotes ATP synthesis possibly helping the rapid repair of photodamaged photosystem II at low light. *Front Plant Sci* 9:239
- Huang S, Zuo T, Ni W (2020) Important roles of glycinebetaine in stabilizing the structure and function of the photosystem II complex under abiotic stresses. *Planta* 251:36
- Jin SH, Li XQ, Hu JY, Wang JG (2009) Cyclic electron flow around photosystem I is required for adaptation to high temperature in a subtropical forest tree, *Ficus concinna*. *J Zhejiang Univ Sci* 10:784–790
- Johnson GN (2011) Physiology of PSI cyclic electron transport in higher plants. *BBA Bioenerget* 18073:384–389
- Joliot P, Johnson GN (2011) Regulation of cyclic and linear electron flow in higher plants. *Proc Natl Acad Sci USA* 10832:13317–13322
- Kudoh H, Sonoike K (2002) Irreversible damage to photosystem I by chilling in the light: cause of the degradation of chlorophyll after returning to normal growth temperature. *Planta* 215:541–548
- Li MF, Li ZM, Li SF, Guo SJ, Meng QW, Li G, Yang XH (2014) Genetic engineering of glycinebetaine biosynthesis reduces the heat-enhanced photoinhibition by enhancing antioxidative defense and alleviating lipid peroxidation in tomato. *Plant Mol Biol Rep* 32:42–51
- Li CY, Zhang TP, Feng PW, Li DX, Brestic M, Liu Y, Yang XH (2021a) Genetic engineering of glycinebetaine synthesis enhances cadmium tolerance in *BADH*-transgenic tobacco plants via reducing cadmium uptake and alleviating cadmium stress damage. *Environ Exp Bot* 191:104602
- Li DX, Wang MW, Zhang TP, Chen X, Li CY, Liu Y, Brestic M, Chen THH, Yang XH (2021b) Glycinebetaine mitigated the photoinhibition of photosystem II at high temperature in transgenic tomato plants. *Photosynth Res* 147:301–315
- Lichtenthaler H, Wellburn A (1983) Determination of total carotenoids and chlorophylls a and b of leaf in different solvents. *Biochem Soc Trans* 11:591–592
- Lima-Melo Y, Alencar VTCB, Lobo AKM, Sousa RHV, Tikkanen M, Aro EM, Silveira JAG, Gollan PJ (2019) Photoinhibition of photosystem I provides oxidative protection during imbalanced photosynthetic electron transport in *Arabidopsis thaliana*. *Front Plant Sci* 10:916
- Maehly AC, Chance B (2006) The assay of catalases and peroxidases. *Methods Biochem Anal* 1:357–424
- Ming R, Zhang Y, Wang Y, Khan M, Dairo B, Liu JH (2021) The JA-responsive *MYC2-BADH-like* transcriptional regulatory module in *Poncirus trifoliata* contributes to cold tolerance by modulation of glycine betaine biosynthesis. *New Phytol* 229:2730–2750
- Montepietra D, Bellingeri M, Ross AM, Scotognella F, Cassi D (2020) Modelling photosystem I as a complex interacting network. *J R Soc Interface* 17:20200813
- Murata N, Nishiyama Y (2018) ATP is a driving force in the repair of photosystem II during photoinhibition. *Plant Cell Environ* 412:285–299
- Murata N, Takahashi S, Nishiyama Y, Allakhverdiev SI (2007) Photoinhibition of photosystem II under environmental stress. *BBA Bioenerget* 1767:414–421
- Nishiyama Y, Murata N (2014) Revised scheme for the mechanism of photoinhibition and its application to enhance the abiotic stress tolerance of the photosynthetic machinery. *Appl Microbiol Biotechnol* 9821:8777–8796
- Ogawa KI, Kanematsu S, Asada K (1997) Generation of superoxide anion and localization of CuZn-superoxide dismutase in the vascular tissue of spinach hypocotyls: their association with lignification. *Plant Cell Physiol* 38:1118–1126
- Ohnishi N, Murata N (2006) Glycinebetaine counteracts the inhibitory effects of salt stress on the degradation and synthesis of D1 protein during photoinhibition in *Synechococcus* sp. PCC 7942. *Plant Physiol* 1412:758–765
- Park EJ, Jeknić Z, Sakamoto A, DeNoma J, Yuwansiri R, Murata N, Chen THH (2004) Genetic engineering of glycinebetaine synthesis in tomato protects seeds, plants, and flowers from chilling damage. *Plant J* 40:474–487
- Park EJ, Jeknić Z, Chen THH (2006) Exogenous application of glycinebetaine increases chilling tolerance in tomato plants. *Plant Cell Physiol* 47:706–714
- Perreault F, Dionne J, Didur O, Juneau P, Popovic R (2011) Effect of cadmium on photosystem II activity in *Chlamydomonas reinhardtii*: alteration of O–J–I–P fluorescence transients indicating the change of apparent activation energies within photosystem II. *Photosynth Res* 107:151–157
- Rhodes D, Rich PJ, Brunk DG, Ju GC, Rhodes JC, Pauly MH, Hansen LA (1989) Development of two isogenic sweet corn hybrids differing for glycinebetaine content. *Plant Physiol* 91:1112–1121
- Roach T, Krieger-Liszky A (2014) Regulation of photosynthetic electron transport and photoinhibition. *Curr Protein Pept Sci* 154:351–362
- Salvatori E, Fusaro L, Gottardini E, Pollastrini M, Goltsev V, Strasser RJ, Bussotti F (2014) Plant stress analysis: application of prompt, delayed chlorophyll fluorescence and 820 nm modulated reflectance. Insights from independent experiments. *Plant Physiol Biochem* 85:105–113
- Sasi S, Venkatesh J, Daneshi RF, Gururani MA (2018) Photosystem II extrinsic proteins and their putative role in abiotic stress tolerance in higher plants. *Plants Basel* 74:100
- Schägger H, von Jagow G (1991) Blue native electrophoresis for isolation of membrane protein complexes in enzymatically active form. *Anal Biochem* 199:223–231
- Solymosi D, Nikkanen L, Muth-Pawlak D, Fitzpatrick D, Vasudevan R, Howe CJ, Lea-Smith DJ, Allahverdiyeva Y (2020) Cytochrome c_M decreases photosynthesis under photomixotrophy in *Synechocystis* sp. PCC 6803. *Plant Physiol* 183:700–716
- Sonoike K, Kamo M, Hihara Y, Hiyama T, Enami I (1997) The mechanism of the degradation of psaB gene product, one of the photosynthetic reaction center subunits of photosystem I, upon photoinhibition. *Photosynth Res* 53:55–63

- Strasser RJ, Tsimilli-Michael M, Qiang S, Goltsev V (2010) Simultaneous *in vivo* recording of prompt and delayed fluorescence and 820-nm reflection changes during drying and after rehydration of the resurrection plant *Haberlea rhodopensis*. *Biochim Biophys Acta (BBA) Bioenerget* 1797:1313–1326
- Strauss AJ, Krüger GHJ, Strasser RJ, Heerden PDRV (2006) Ranking of dark chilling tolerance in soybean genotypes probed by the chlorophyll a fluorescence transient o–j–i–p. *Environ Exp Bot* 562:147–157
- Tadmor Y, Raz A, Reikin-Barak S, Ambastha V, Shemesh E, Leshem Y, Crane O, Stern RA, Goldway M, Tchernov D, Liran O (2021) Metamitron, a photosynthetic electron transport chain inhibitor, modulates the photoprotective mechanism of apple trees. *Plants (basel)* 10:2803
- Takahashi S, Milward SE, Fan DY, Chow WS, Badger MR (2009) How does cyclic electron flow alleviate photoinhibition in *Arabidopsis*? *Plant Physiol* 149:1560–1567
- Thierry J, Cournac L, Peltier G, Havaux M (2002) Cyclic electron flow around photosystem I in C3 plants. In vivo control by the redox state of chloroplasts and involvement of the NADH-dehydrogenase complex. *Plant Physiol* 128:760–769
- Tikkanen M, Mekala NR, Aro EM (2014) Photosystem II photoinhibition–repair cycle protects photosystem I from irreversible damage. *BBA Bioenerget* 1837:210–215
- Wang P, Duan W, Takabayashi A, Endo T, Shikanai T, Ye JY, Mi H (2006) Chloroplastic NAD(P)H dehydrogenase in tobacco leaves functions in alleviation of oxidative damage caused by temperature stress. *Plant Physiol* 141:465–474
- Wang F, Wu N, Zhang LY, Ahammed GJ, Chen XX, Zhou J, Xia XJ, Shi K, Yu JQ, Foyer CH, Zhou YH (2018) Light signaling-dependent regulation of photoinhibition and photoprotection in tomato. *Plant Physiol* 176:1311–1326
- Wang F, Yan J, Ahammed GJ, Wang X, Bu X, Xiang H, Li Y, Lu J, Liu Y, Qi H, Qi M, Li T (2020) PGR5/PGRL1 and NDH mediate far-red light-induced photoprotection in response to chilling stress in tomato. *Front Plant Sci* 11:669
- Wei DD, Zhang W, Wang CC, Meng QW, Li G, Chen THH, Yang XH (2017) Genetic engineering of the biosynthesis of glycinebetaine leads to alleviate salt-induced potassium efflux and enhances salt tolerance in tomato plants. *Plant Sci* 257:74–83
- Yamori W, Shikanai T (2016) Physiological functions of cyclic electron transport around photosystem I in sustaining photosynthesis and plant growth. *Annu Rev Plant Biol* 67:81–106
- Yang XH, Liang Z, Lu CM (2005) Genetic engineering of the biosynthesis of glycinebetaine enhances photosynthesis against high temperature stress in transgenic tobacco plants. *Plant Physiol* 138:299–309
- Yang XH, Wen XG, Gong HM, Lu QT, Yang ZP, Tang YL, Liang Z, Lu CM (2007) Genetic engineering of the biosynthesis of glycinebetaine enhances thermotolerance of photosystem II in tobacco plants. *Planta* 225:719–733
- Yang XH, Liang Z, Wen XG, Lu CM (2008) Genetic engineering of the biosynthesis of glycinebetaine leads to increased tolerance of photosynthesis to salt stress in transgenic tobacco plants. *Plant Mol Biol* 66:73–86
- Zeng R, Li Z, Shi Y, Fu D, Yin P, Cheng J, Jiang C, Yang S (2021) Natural variation in a type-A response regulator confers maize chilling tolerance. *Nat Commun* 12:4713
- Zhang L, Paakkarinen V, van Wijk KJ, Aro EM (1999) Co-translational assembly of the D1 protein into photosystem II. *J Biol Chem* 274:16062–16067
- Zhang TP, Li ZM, Li DX, Li CY, Wei DD, Li SF, Liu Y, Chen THH, Yang XH (2020) Comparative effects of glycinebetaine on the thermotolerance in *codA*- and *BADH*-transgenic tomato plants under high temperature stress. *Plant Cell Rep* 39:1525–1538
- Zhang TP, Zhang WX, Li DX, Zhou FL, Chen X, Li CY, Yu S, Brestic M, Liu Y, Yang XH (2021) Glycinebetaine: a versatile protectant to improve rice performance against aluminium stress by regulating aluminium uptake and translocation. *Plant Cell Rep* 40:2397–2407
- Zhu JK (2016) Abiotic stress signaling and responses in plants. *Cell* 167:313–324

Publisher's Note Springer Nature remains neutral with regard to jurisdictional claims in published maps and institutional affiliations.

Authors and Affiliations

Dandan Wei^{1,2} · Tianpeng Zhang¹ · Bingquan Wang³ · Huiling Zhang¹ · Mingyang Ma¹ · Shufen Li¹ · Tony H. H. Chen⁴ · Marian Brestic⁵ · Yang Liu¹ · Xinghong Yang¹ 

Dandan Wei
1246270136@qq.com

Tianpeng Zhang
zhangtianpeng0718@163.com

Bingquan Wang
2069377077@qq.com

Huiling Zhang
huiling900120@163.com

Mingyang Ma
1054183671@qq.com

Shufen Li
shufenlili@163.com

Tony H. H. Chen
tony3hchen@gmail.com

Marian Brestic
marian.brestic@uniag.sk

¹ College of Life Science, State Key Laboratory of Crop Biology, Shandong Key Laboratory of Crop Biology, Shandong Agricultural University, Taian 271018, Shandong, China

² Xinzhou Teachers University, Xinzhou 034000, Shanxi, China

³ Maize Research Institution, Shanxi Academy of Agricultural Sciences, Xinzhou Shanxi 034000, China

⁴ Department of Horticulture, Oregon State University, ALS 4017, Corvallis, OR 97331, USA

⁵ Department of Plant Physiology, Slovak University of Agriculture, A. Hlinku 2, Nitra 94976, Slovak Republic